Journal of Molecular Graphics and Modelling 28 (2010) 446–454

Contents lists available at ScienceDirect

Journal of Molecular Graphics and Modelling

journal homepage: www.elsevier.com/locate/JMGM

Characterization of the conformational ensemble from bioactive *N*-acylhydrazone derivatives

Laercio Pol-Fachin [a], Carlos Alberto Massour Fraga [c,d], Eliezer J. Barreiro [c,d], Hugo Verli [a,b,*]

[a] *Programa de Pós-Graduação em Biologia Celular e Molecular, Centro de Biotecnologia, Universidade Federal do Rio Grande do Sul, Av. Bento Gonçalves 9500, CP 15005, Porto Alegre 91500-970, RS, Brazil*
[b] *Faculdade de Farmácia, Universidade Federal do Rio Grande do Sul, Av. Ipiranga 2752, Porto Alegre 90610-000, Rio Grande do Sul, RS, Brazil*
[c] *Laboratório de Avaliação e Síntese de Substâncias Bioativas (LASSBio), Faculdade de Farmácia, Universidade Federal do Rio de Janeiro, PO Box 68023, Rio de Janeiro 21941-902, RJ, Brazil*
[d] *Programa Pós-Graduação em Química, Instituto de Química, Universidade Federal do Rio de Janeiro, RJ, Brazil*

ARTICLE INFO

Article history:
Received 9 June 2009
Received in revised form 15 October 2009
Accepted 21 October 2009
Available online 30 October 2009

Keywords:
Conformational analysis
GROMACS
LASSBio-294
Molecular dynamics
N-Acylhydrazone

ABSTRACT

The search for bioactive conformations from prototypes is mostly referenced on crystallographic ligand–receptor complexes, in which the molecule conformation is already caged inside its binding site. However, the complexation process is a thermodynamic event depending on both complexed and uncomplexed states. As ligand affinity originates from such equilibrium, the development of novel computational models capable of supplying data on ligand dynamics in biological solutions is potentially applicable in more efficient methods for prediction of compounds binding and affinity. In this context, the current work employs a series of molecular dynamics simulations on three *N*-acylhydrazone derivatives, already shown to present promising cardioinotropic and vasodilatory activities, in order to obtain a precise characterization of each compound conformational ensemble in aqueous solutions, instead of a single minimum energy conformation. Consequently, we were able to observe the influence of each functional group of the studied molecules on the conformation of the entire compounds and thus on the exposure of functional groups that might potentially bind to target receptors. Additionally, the differences between the molecules conformational behavior were characterized, supporting a spatial and temporal image of each ligand, which may be potentially correlated to their biological activities. So in the context of conformational selection, such strategy may represent a useful methodology to contribute in the choice of ligands conformations for both 3D-QSAR and docking calculations.

1. Introduction

An important strategy in medicinal chemistry efforts to develop new bioactive compounds is the identification of the pharmacophore, a structural framework that comprises stereoelectronic properties and three-dimensional characteristics necessary to the complexation of ligands to a specific target receptor [1] and, consequently, to initiate a set of activities. An example of such group may be found in the *N*-acylhydrazone (NAH) moiety, already shown to be related to a series of biological activities such as analgesic, anti-inflammatory, and platelet aggregation inhibition activities [2–10], as well as protozoa proteases inhibition [11], HIV-1 reverse transcriptase dimmer destabilization [12], antibiotic and antifungal activities [13], and cardiovascular actions [14–18]. The prototype of this class of compounds, LASSBio-294, was first synthesized from natural safrole and identified as a potential alternative therapeutic for congestive heart failure due to a positive cardioinotropic effect through an interaction with the Ca^{2+} uptake/release process of the sarcoplasmic reticulum [14,15,17]. More recently, a vasodilatory action was also observed [16].

These diverse biological activities appear to be related to the same pharmacophoric group (in each case, added by specific substituents), rendering to the NAH moiety the status of privileged structure [7]. However, its conformational characterization as a function of biological solutions and specific or non-specific target receptors is highly difficult to be obtained under experimental techniques, as NMR and X-ray crystallography, due to few inter-proton distances and potential crystal packing effects [19,20].

One strategy usually employed attempting to circumvent such limitations in the conformational description of bioactive compounds consists in performing a conformational analysis. While

* Corresponding author at: Faculdade de Farmácia, Universidade Federal do Rio Grande do Sul, Av. Ipiranga 2752, Porto Alegre 90610-000, Rio Grande do Sul, RS, Brazil. Tel.: +55 51 3308 7770; fax: +55 51 3308 7309.
E-mail address: hverli@cbiot.ufrgs.br (H. Verli).
URL: http://www.cbiot.ufrgs.br/bioinfo

1093-3263/$ – see front matter © 2009 Elsevier Inc. All rights reserved.
doi:10.1016/j.jmgm.2009.10.004

such method, in its myriad of possible strategies, is usually concerned in medicinal chemistry to search for minimum energy structures, simulation techniques as molecular dynamics (MD) generate an ensemble of conformational states that include structures not at its energy minima [21]. The reliability of models built using computer simulation techniques depends mostly on (1) the size of the configurational space simulated, and (2) the accuracy of the force field employed to model the molecular system [22]. As a consequence, a tradeoff may be observed between accuracy of the force field on the one hand and the time scale that can be attained on the other. When properly validated, the additional kinetic energy due to temperature enhances the ability of the system to explore its potential energy surface and thus prevent the molecule to stay trapped in a localized region of the conformational space [21]. In this process, the explicit inclusion of solvent effects, as well as the evaluation of compounds conformation as an ensemble, supports their conformational description closer to a biological solution environment.

In this context, the current work intends to obtain a conformational characterization of the cardio- and vasoactive 2-thienylidene *N*-acylhydrazone derivatives LASSBio-294 (**1**) and LASSBio-785 (**3**) in explicit solvent, comparing their behavior with that displayed by furylidene isoster LASSBio-129 (**2**) [23]. Globally, the obtained results indicate that the conformational analysis of compounds, integrating quantum mechanical and simulation methods to consider both spatial and temporal components, may represent a promising tool for describing compounds conformational ensemble in biological solutions. Ultimately, it may contribute in building more accurate pharmacophoric models and, consequently, in an increased understanding of structure–activity relationships.

2. Experimental

2.1. Software

The compounds topologies were generated with the PRODRG server [24], the *ab initio* calculations were performed using GAMESS [25], the semi-empirical calculations were performed using MOPAC2009 [26], manipulation of structures was performed with MOLDEN [27], and all the MD calculations and analysis were performed using the GROMACS simulation suite [28] and GROMOS96 force field [29], as an inexpensive and fast simulation package.

2.2. Conformational analysis strategy

In order to obtain a detailed picture of NAH conformational features, as well as its dependence on bounded substituents, the molecules (Fig. 1) were divided as building blocks (named blocks I–III) [30]. Such strategy intends to support both the conformational characterization of the NAH derivatives, with a progressive level of complexity, and the isolation of specific conformational attributes added by each of the compounds functional groups. In this context, block I is composed by the NAH unit or by the *N*-methyl-*N*-acylhydrazone unit (NMNAH), whose degrees of freedom were named ϕ_1 and ϕ_2 (Fig. 2 A). The inclusion of the 1,3-benzodioxolyl ring on such moieties added the ϕ_3 dihedral and defined block II (Fig. 2B). Finally, the addition of 2-thienyl or 2-furyl rings created the ϕ_4 dihedral, and this complete form of the compounds was named block III (Fig. 3C). Additionally, as the synthesis of NAH derivatives is described to produce mainly the (*E*)-diastereoisomers [4,18,23], only the isomer presenting this relative configuration was considered for the studied compounds. Based on this fragmentation strategy, each of the above-mentioned degrees of freedom was sampled by semi-empirical calculations to accordingly include quantum mechanical parameters. In sequence, each of these minimum energy conformations was submitted to microsecond MD simulations in explicit solvent in order to describe the conformational behavior of each molecule in aqueous solutions. The details of these proceedings are described below in the text.

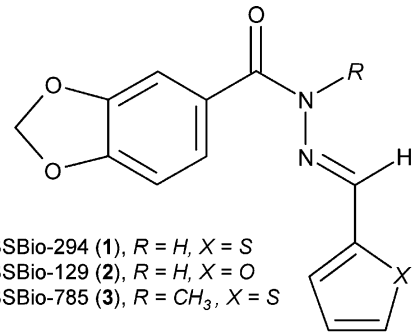

LASSBio-294 (**1**), *R* = *H*, *X* = *S*
LASSBio-129 (**2**), *R* = *H*, *X* = *O*
LASSBio-785 (**3**), *R* = CH_3, *X* = *S*

	1	2	3
Vasodilatory (IC_{50})	74 μM	*n.d.*	10.2 ± 0.5 μM
Analgesic (ID_{50})	8.1 μmol.kg^{-1}	*n.d.*	*n.d.*
Anti-platelet (IC_{50})	15.3 μM	*n.d.*	*n.d.*
Anti-inflamatory (% of inhibition)	29.7	*n.d.*	*n.d.*

n.d. = not determined;

Fig. 1. The structure of the studied molecules: LASSBio-294 (**1**), LASSBio-129 (**2**) and LASSBio-785 (**3**), together with their biological activities, as determined [7,10,16,18].

2.3. Search for minimum energy conformations on each block

The structures in each of the three above-mentioned blocks (Fig. 2) were submitted to full-geometry optimization using RM1 Hamiltonian semi-empirical method [31] at the SCF-MO level in the gas phase with MOPAC2009. Hessian matrix analyses were employed to unequivocally characterize the obtained geometries as true minima potential energy surface [32]. Each degree of freedom, as identified in Fig. 2, was rotated from 0 to 360° with a 30° step. The obtained conformers were energy optimized using restraints only for the studied dihedrals, allowing the rest of the molecule to be minimized. The use of RM1 semi-empirical calculations, as well as other newer Hamiltonians, PM6, support a fast geometry optimization and account for high resolution structures, frequently in best agreement to experimental data then high level Hartree–Fock calculations [33–35]. Additionally, systems composed by compounds **1**–**3** in the presence of explicit water molecules, obtained from MD simulations, were submitted to geometry optimization under MOZYME procedure. For comparison, all semi-empirical calculations in the absence of explicit solvent molecules were also performed under PM6 method [36] and under COSMO continuum model [37] (supplementary data).

2.4. MD simulations

The minimum energy conformations obtained from RM1 semi-empirical calculations were used as starting points for a series of MD simulations. Such structures were submitted to the PRODRG site, and the initial geometries and crude topologies under the GROMOS96 force field were retrieved. These topologies were modified to include atomic charges following a proceeding previously described by our group [38–40]. Such protocol was shown to be able to offer an adequate conformational representation of highly charged compounds as carbohydrates and glycosaminoglycans, as well as its binding to target receptors, with a lower

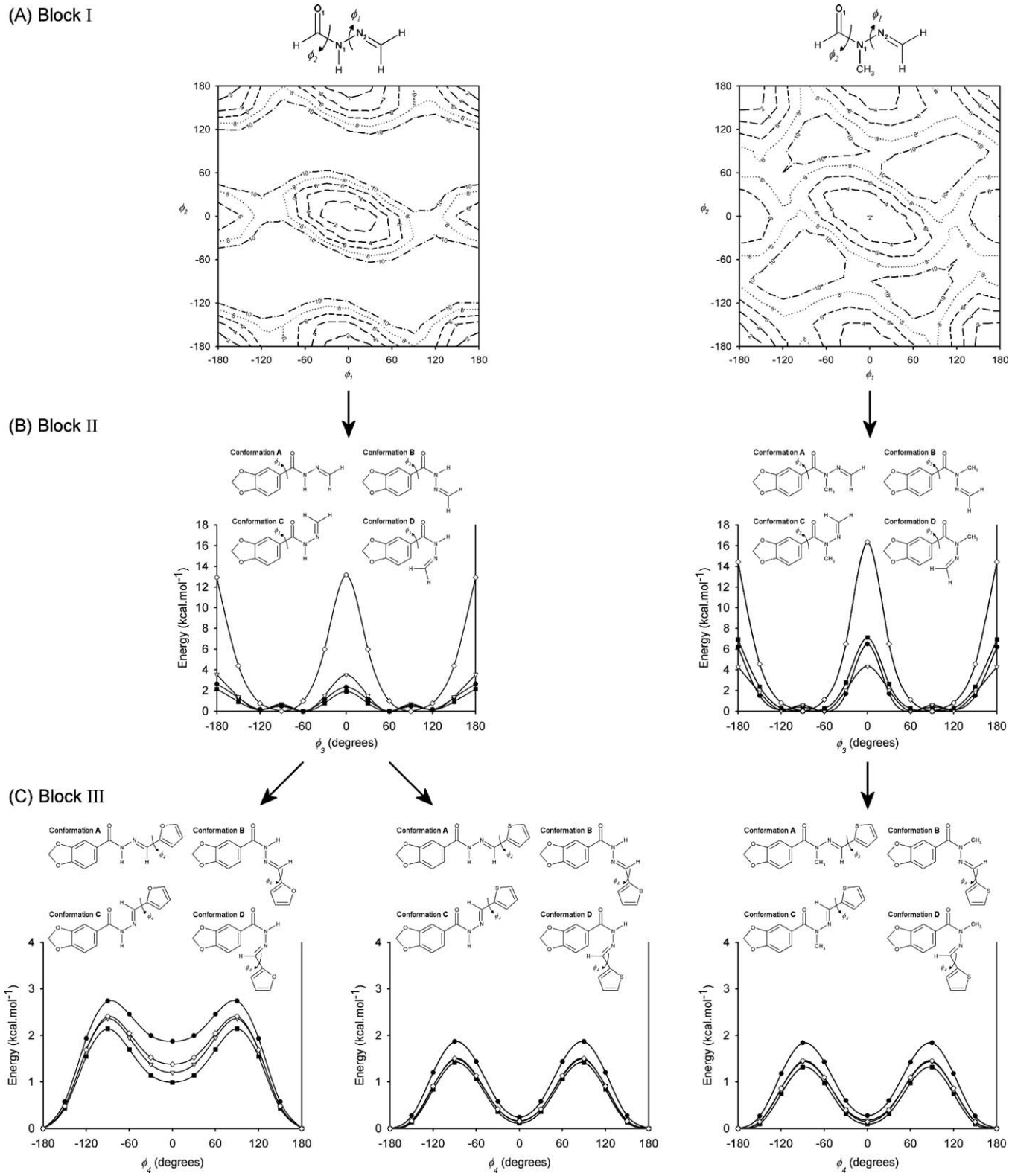

Fig. 2. Semi-empirical conformational analysis of the studied compounds. In (A), energy maps for the rotation of ϕ_1 and ϕ_2 are presented with contour levels shown at every 2 kcal mol^{-1} from 2 to 10 kcal mol^{-1}. In (B) and (C), the energy calculation (RM1) for the rotation of ϕ_3 and ϕ_4 is plotted as a function of NAH and NMNAH conformation: A (closed circles), B (open triangles), C (closed squares) and D (open diamonds).

influence of compounds conformation on the obtained atomic charge values, as expected to occur using electrostatic derived atomic charges. Such conformational effects are potentially serious in flexible compounds containing polar functional groups, as in the case of the studied NAH derivatives. Briefly, the atomic charges were generated through a full-geometry optimization at the HF/3-21G level with GAMESS, followed by a HF/6-31G** level optimization to obtain Löwdin atomic charges (included in supplementary data). Additionally, the energy barriers obtained form such topologies in vacuum were validated upon comparison

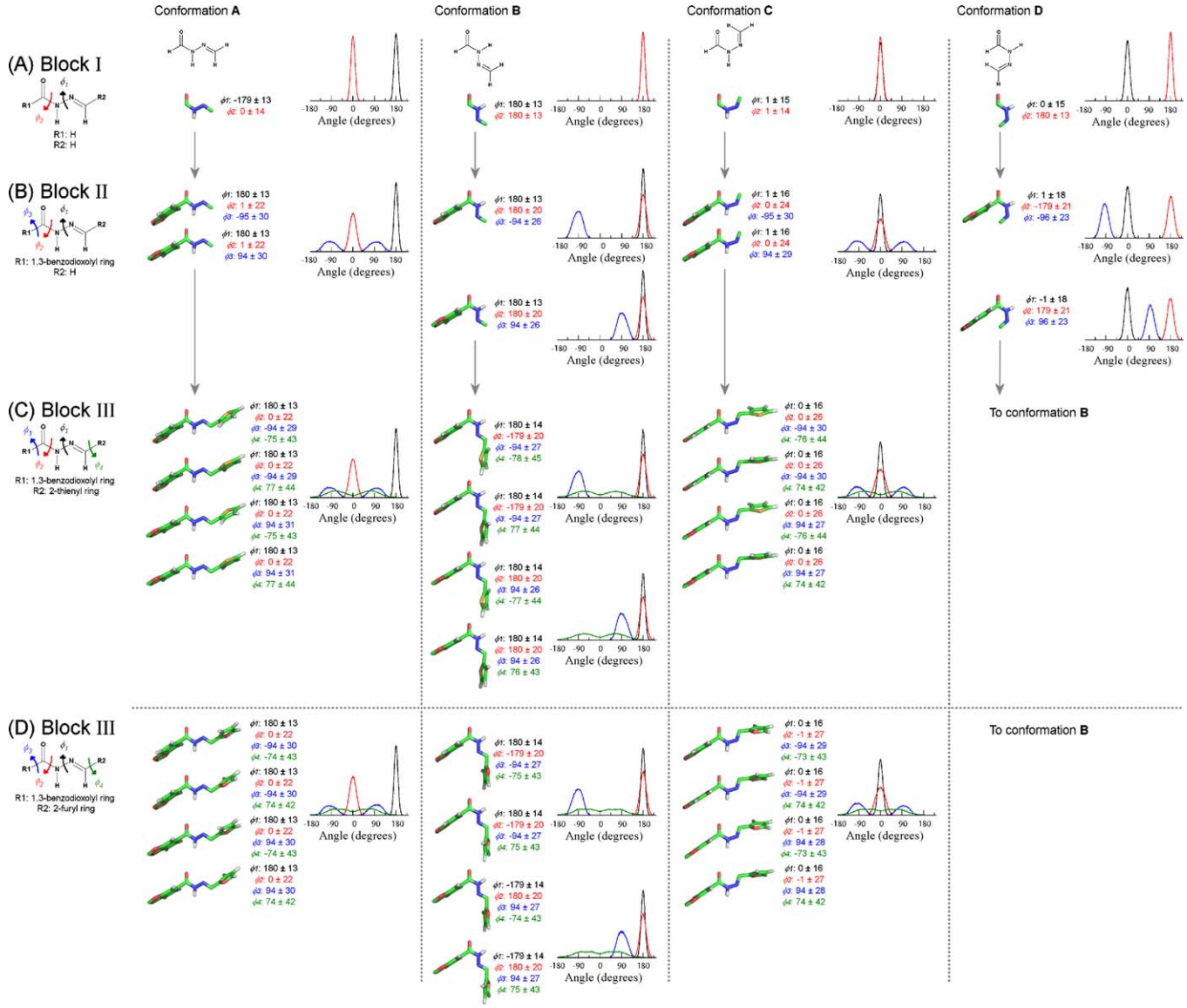

Fig. 3. MD conformational analysis of compounds **1** and **2**. The distribution curves show the solution behavior of ϕ_1 (black), ϕ_2 (red), ϕ_3 (blue) and ϕ_4 (green), while the structures demonstrate the possible conformers on the three blocks of MD simulations (geometry of each conformer presented beside its structure). While block I (A) and block II (B) are equivalent in compounds **1** and **2**, (C) represents block III of **1** and (D) correspond to block III of **2**.

to the barriers obtained from semi-empirical calculations (supplementary data).

The minimum energy geometries from semi-empirical calculations, described through GROMOS96 topologies, were solvated in rectangular boxes using periodic boundary conditions with a 10 Å minimum distance from solute to the box faces and the SPC [41] water model. These systems were submitted to MD simulations for 0.1 μs, employing a protocol based on previous studies [42] after an energy minimization step with Steepest Descents algorithm. No additional heating period was performed. All simulations applied the Particle-Mesh Ewald method [43] with Coulomb and van der Waals cut-offs adjusted to 9 Å. The Lincs method [44] was applied to constrain covalent bond lengths, allowing an integration step of 2 fs. Temperature and pressure were kept constant at 1.0 atm and 310 K by coupling compounds and solvent to external temperature and pressure baths under Berendsen-thermostat with coupling constants of $\tau = 0.1$ and 0.5 ps [45], respectively. The dielectric constant was treated as $\varepsilon = 1$, and the reference temperature adjusted to 310 K. The structure of the solvent around the studied molecules was analyzed through calculation of radial distribution functions [28], solvent molecules orientation [28] and water residence times [40]. The simulations data were collected at every 250 ps, while the analyses were performed under all trajectories. The simulations equilibrium was evaluated by accompanying standard physical chemical parameters of the systems as volume, density, pressure, temperature, and energy terms.

3. Results and discussion

3.1. Dynamics of NAH and NMNAH

Considering the role of NAH as a pharmacophoric group involved in diverse biological activities, the comprehension of its conformational behavior is potentially capable to contribute in the understanding of its binding to distinct target receptors. As shown in Fig. 2A, the RM1 calculations, combining the conformational preferences of both ϕ_1 and ϕ_2 dihedral angles, suggest that the NAH unit presents four main conformations in the gas phase, named by us A ($\phi_1 = 180°$; $\phi_2 = 0°$), B ($\phi_1 = 180°$; $\phi_2 = 180°$), C ($\phi_1 = 0°$; $\phi_2 = 0°$) and D ($\phi_1 = 0°$; $\phi_2 = 180°$). These conformational states

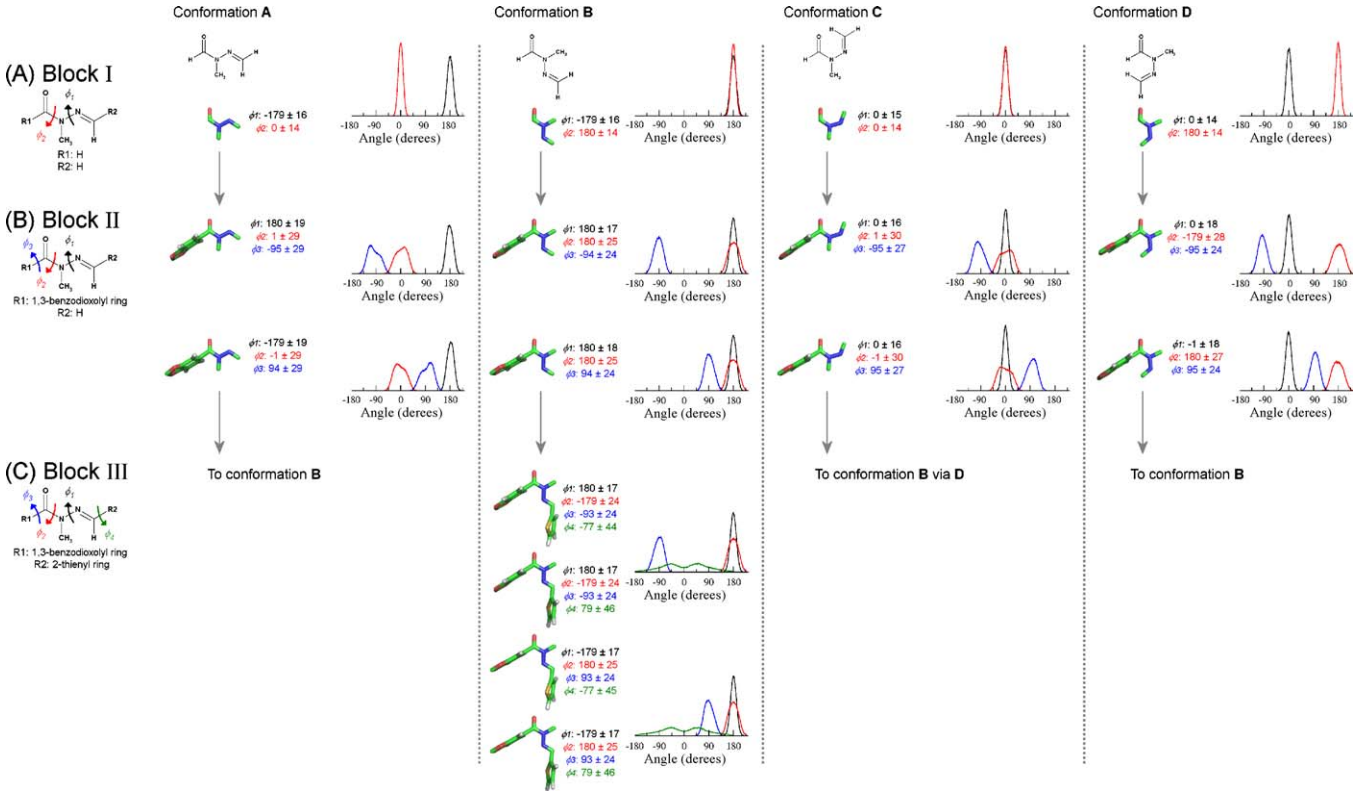

Fig. 4. MD conformational analysis of compound **3**. The distribution curves show the solution behavior of ϕ_1 (black), ϕ_2 (red), ϕ_3 (blue) and ϕ_4 (green), while the structures demonstrate the possible conformers on the three blocks of MD simulations (geometry of each conformer presented beside its structure).

were previously observed in similar compounds, employing the AM1 force field, upon salicylaldehyde *N*-acylhydrazones [46]. The energy barriers between these states, from 8 to 25 kcal mol^{-1}, indicate considerable restrictions for the free rotation of the dihedrals composing such group (Fig. 2A), *i.e.* forbidding a prompt conversion between these four conformational states. As a consequence, it suggests that the NAH pharmacophoric group could exist, simultaneously, in four minimum energy conformational states. However, such observations were based on the gas phase, which does not consider the explicit influence of solvent. So, in order to verify the stability of conformations A-D from NAH skeleton in biological solutions, such states were submitted to MD simulations in water. During these simulations, the solvent was not capable to further modify the distribution of the A–D conformational states neither promote conversions between them in the simulated time scales (up to 0.4 μs), reinforcing the notion that the NAH moiety, while being a pharmacophoric group employed in drug design, should be considered as a structure containing at least four main conformational states (Fig. 3A).

Recently, some new derivatives of compound **1** were designed by performing modifications in the stereoelectronic behavior of the NAH moiety [18]. In this context, compound **3** was synthesized employing **1** as a precursor through *N*-alkylation with a methyl group in the amide subunit of NAH framework, forming an NMNAH derivative. Such compound showed to be seven times more potent than its precursor in reducing the phenylephrine-induced contracture in aortic rings, *i.e.* to stimulate vasodilation [18]. However, it is unclear if such modifications are caused by the inclusion of new interactions with the target receptor or by conformational modifications in the ligand. Therefore, in order to characterize the conformational preferences of NMNAH, from compound **3**, in comparison to NAH, from compounds **1** and **2**, we have performed the same semi-empirical and MD analysis for this pharmacophoric group.

NMNAH, similarly to NAH, showed four main conformational states, comparable to the previously obtained for its non-methylated derivative (Figs. 1 and 3A), named likewise as "A" ($\phi_1 = 180°; \phi_2 = 0°$), "B" ($\phi_1 = 180°; \phi_2 = 180°$), "C" ($\phi_1 = 0°; \phi_2 = 0°$) and "D" ($\phi_1 = 0°; \phi_2 = 180°$). According to RM1 calculations, the energy barriers associated with the rotation of dihedrals ϕ_1 and ϕ_2 are lower in NMNAH than those observed for NAH, from 6 to 15 kcal mol^{-1}. Still, such differences do not confer a higher probability of conversion between these conformational states, as it may be observed by its high stability during MD simulations (Fig. 4 A). Accordingly, such group should also be considered as containing at least four main conformational states.

3.2. Dynamics of substituted NAH and NMNAH

The identification of NAH and NMNAH conformational preferences in solution may be considered as a step towards the understanding of their recognition by target receptors (see further in the text). However, these pharmacophoric frameworks are usually connected to other groups, which may promote conformational restrictions or inductions on the A–D conformations above observed. So, in order to obtain insights into the influence of substituents on NAH and NMNAH conformations, the following items will depict the effect of substitutions at both acyl and imine sub-unities of these pharmacophoric groups.

3.2.1. Substitutions at the acyl subunit

The studied *N*-acylhydrazone derivatives, that is, compounds **1**–**3**, present a single group modifying the acyl subunit, the 1,3-benzodioxolyl ring. Under RM1 semi-empirical calculations, depending on the input conformation of the NAH nucleus, two distinct behaviors were observed: one, for NAH conformations A–C, with a ϕ_3 rotational barrier lower than 4 kcal mol^{-1} (Fig. 2B) and other, achieved by NAH conformation D, which presented a ϕ_3

rotational barrier of about 13 kcal mol^{-1} (Fig. 2B). The gas phase minimum energies on these degrees of freedom were similar, independently on the NAH conformation attached to the 1,3-benzodioxolyl ring (Fig. 2B) or on the semi-empirical method employed (supplementary data), with the distinction of a possible ϕ_3 steric hindrance when NAH lies at its D geometry.

Accordingly, each of the obtained minimum energy conformations was further submitted to refinements under MD simulations in the presence of explicit solvent. The first important observation to be noted, based on these simulations, points to the substitution of the 1,3-benzodioxolyl ring at the acyl subunit of NAH moiety, which did not promote conformational modifications in NAH solution ensemble (Fig. 3B), in spite of the ring volume. The only observable modification is a slight increase (*i.e.* widening of the distribution curve base) in flexibility around ϕ_2, independently on the NAH conformation. On the other hand, concerning ϕ_3 conformational behavior, two distinct profiles were observed in the performed simulations: (1) when the NAH conformation lies in states A and C, a prompt equilibrium is achieved between the two gas phase minimum energy states, around 90° and −90°, indicating a free rotation of the 1,3-benzodioxolyl ring; (2) when the NAH conformation lies in states B and D, the energy barrier around ϕ_3 avoids such equilibrium, sustaining two conformational states, as derived from its gas phase minimum energy conformations, around 90° or around −90° (Fig. 3B and supplementary data). While the MD conformational behavior is mostly in accordance to the gas phase calculations, one exception is worth to be noted. While the NAH conformation B presents a ϕ_3 energy barrier similar to the ones shown by conformations A and C, its ensemble pattern in aqueous solution is more similar to that presented by conformation D, which presents an energy barrier more than three times higher (Fig. 2B). In fact, as it will be observed further in the text, such behavior appears to be directly dependent on the surrounding solvent structure and dynamics.

Concerning the 1,3-benzodioxolyl ring rotation on NMNAH, as observed for NAH, two main conformations are observed for ϕ_3, around 90° and −90° (Fig. 2B), according to RM1 calculations. However, the addition of an *N*-methyl group promoted a significant increase in ϕ_3 energy barrier (Fig. 2B), adding some level of rigidity at this region of the compounds. Such pattern is clearly observed during MD, as no conversion between the two conformational states of ϕ_3 angle is observed in the simulation time (Fig. 4B). As a consequence, it may be expected a lower amount of compounds prompt to fit the target receptor, as larger amounts of energy would be necessary to convert one conformational state to other. On the other hand, given the increased rigidity, it may offer thermodynamic contributions to the interaction by lowering the entropic cost of binding depending on the receptor requirements.

3.2.2. Substitutions at the imine subunit

The preferred conformations from block II were added by 2-thienyl or 2-furyl rings substitutions at the NAH imine subunit, producing block III structures (Fig. 2C). Therefore, the main conformational states assumed by simpler building blocks in aqueous solution are employed as the starting points for the construction of larger molecules. The new group is added using gas phase minimum energy conformations as starting geometries, being further refined in 0.1 μs MD simulations.

In this context, both 2-thienyl and 2-furyl rings, when bound to NAH, prefer planar orientations at the gas phase (0° and 180°) based on RM1 and PM6 calculations, in vacuum or implicit solvent models (Fig. 2C; supplementary data). Upon addition of explicit solvent on these systems, a similar drift for both 2-thienyl and 2-furyl derivatives was observed toward two main conformational states, −75° and 75° (Fig. 3C and D), suggesting a role of solvation on compounds conformations in biological environments. Moreover, as a consequence of 2-thienyl and 2-furyl rings presence in these molecules, it could be observed a conversion from D to B conformers, for both compounds **1** and **2** (Fig. 3C and D).

As noted from RM1 calculations, very similar energy barriers are obtained for 2-thienyl ring rotation in NMNAH in comparison to NAH (Fig. 2C) and, in aqueous solution, dihedral 4 also showed an equilibrium between conformations around −75° and 75° (Fig. 4C). On the other hand, the NMNAH conformational states A, C, and D converged to the B state.

3.3. Role of solvation on NAH derivatives properties

Solute–solvent interactions are of special interest in biologically active systems [47]. The role of structural waters, as well as solvation effects, is widely described for proteins and other biologically active compounds [40,48–52]. In this context, MD simulations of solutes in water may provide a detailed examination of water–solute interactions [53], such as previously described for nirusidine [54] and heparin [40].

The data described in Figs. 3 and 4 and in supplementary data suggest that compounds **1**–**3** present distinct conformational profiles in aqueous solutions due to its relative abundances during the performed MD calculations. The conformational sampling obtained on these simulations was also capable to describe the conversion between conformational states, that is, unoccupied states shifted towards most favorable ones. Such pattern includes conformation D for compounds **1**–**2**, spontaneously changed to conformation B during simulations, and conformations A, C and D for compounds **3**, all modified to conformation B. These conformational states, populated in solution by compounds **1**–**3**, were also submitted to thermodynamic analysis using the RM1 semi-empirical method (see supplementary data). The so obtained data agrees well to the MD conformational sampling, indicating almost equivalent free-energy values for the conformational states populated by the compounds (differences in free-energy lower than 1.0 kcal mol^{-1}) and, consequently, pointing to the co-existence of three states for compounds **1**–**2**, while compound **3** apparently lies in a single form.

In order to further evaluate the possible roles of solvation on the studied molecules, we analyzed the radial distribution functions (RDF) and water residence times around the NAH and NMNAH polar groups in the compounds **1**–**3**, as well as solvent orientation around oxygen and sulfur atoms in 2-furyl and 2-thienyl rings, as presented in Fig. 5 and Table 1.

The donor and acceptor hydrogen-bond groups present in NAH and NMNAH moieties did not show significant differences in RDF. However, higher water residence times for the carbonyl oxygen O_1 and both N_1 and N_2 in A and C states may be observed in compounds **1** and **2** (Table 1), indicating that such conformers are more tightly bound to water molecules that B. As more intense is the water–solute interaction, higher will be the enthalpic cost for the complex formation and, consequently, different conformational states would probably present different thermodynamic preferences in its interactions with the target receptor.

Comparing the differences between the studied compounds, the methyl group, instead of a hydrogen, in compound **3**, seems to promote a distancing of both nitrogen atoms to the solvent, *i.e.* more remote hydration shells (Fig. 5, red comparing to black and blue curves), and to diminish their water residence times, markedly around N_1 (Table 1). On the other hand, O_1 seems to be slightly more disposed to hydrogen bonds (Table 1) and to present a higher first hydration shell (Fig. 5) in compound **3** than in compounds **1** and **2**.

More interesting, the sulfur atom in compounds **1** and **3** presented similar water residence time (around 3 ps) to that of the

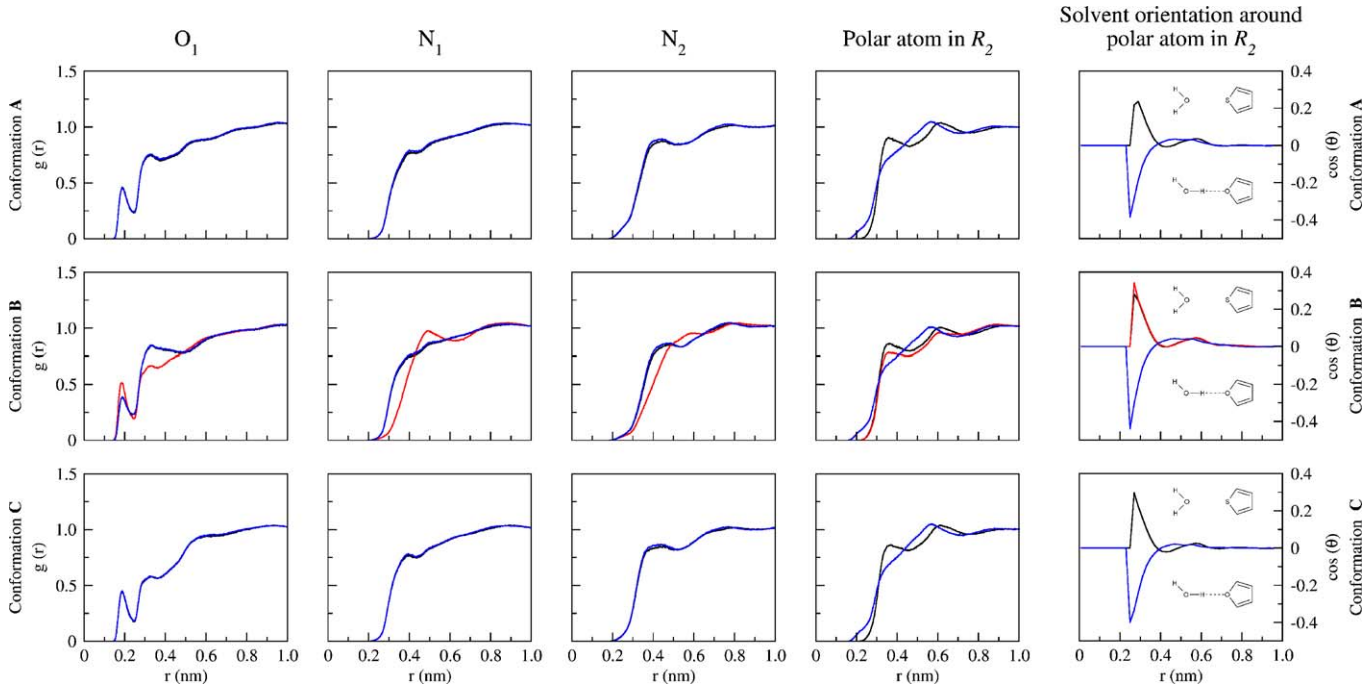

Fig. 5. Radial distribution functions (RDF) of water molecules around polar atoms of NAH and NMNAH moieties of the studied compounds as a function of their conformation and solvent orientation around polar atoms of 2-thienyl and 2-furyl rings.

oxygen atom in compound **2** (approximately 3.3 ps), whereas with a more remote first hydration shell (Fig. 5, black and red compared to blue curves). In addition, the solvent orientation around the sulfur atom in 2-thienyl group from compound **1** indicate that the water molecules in its first hydration orients to the bulk, while the same analysis around the oxygen atom in the 2-furyl moiety from compound **2** suggest solvent molecules pointing toward the compound (Fig. 5). This is an important observation, as the bioisosteric replacement between these two rings does not interfere with the molecules conformational equilibrium, since the ϕ_4 angle, formed by them, present similar geometries (Fig. 3). Nevertheless, it appears to be capable to modify the propensity of each group to interact with their respective target receptor, as the oxygen atom of 2-furyl moiety seems to be more exposed to hydrogen bonds than the sulfur atom in 2-thienyl ring (Fig. 5). These results are in agreement with semi-empirical calculations employing the last MD frame as starting geometry (supplementary data), considering both first solvation sphere and water molecules orientation at the polar atom in R_2 (Fig. 5).

Table 1
Water residence time on the polar atoms that compose NAH and NMNAH moieties during 0.1 μs MD simulations of block III for compounds **1**–**3**.

Compound	Water residence time (ps)[a,b]		
	O_1	N_1	N_2
LASSBio-294 (**1**)			
Conformation A	6.2 ± 0.2	4.5 ± 0.2	3.4 ± 0.2
Conformation B	4.8 ± 0.3	3.2 ± 0.1	2.4 ± 0.0
Conformation C	5.6 ± 0.3	3.5 ± 0.1	3.0 ± 0.1
LASSBio-129 (**2**)			
Conformation A	5.3 ± 0.1	4.3 ± 0.1	3.3 ± 0.0
Conformation B	4.9 ± 0.2	3.0 ± 0.2	2.4 ± 0.1
Conformation C	6.0 ± 0.2	3.6 ± 0.0	3.0 ± 0.0
LASSBio-785 (**3**)			
Conformation B	5.1 ± 0.0	1.4 ± 0.1	1.8 ± 0.0

[a] Values presented as averages ± standard deviations between three water residence time values obtained from MD simulations.
[b] For atoms legend, see Fig. 2.

3.4. Considerations to conformational analysis and design of bioactive compounds

Besides pharmacophoric recognition, the knowledge of the conformational preferences of bioactive compounds, and consequent possible arrangements in physiological solutions, has become an important issue for the comprehension of compounds biological activities, while support the design of new optimized prototypes. In order to obtain such data, experimental procedures, such as X-ray crystallography and NMR techniques, have been widely used to comprehend the conformational preferences of drug-like organic molecules [55]. For NAH derivatives, the results obtained from X-ray crystallography, describing such moiety in a linear form [56], were employed for docking studies [57], as well as for providing insights into their structures in solution [58]. However, such procedures may present some limitations, such as possible crystal packing effects on the molecules and, depending on the crystal environment, conformational states not necessarily correlated to a bioactive conformation [59].

As a consequence, the search for alternative conformational states as a function of the surrounding environment may contribute in achieving a more complete description of molecules conformational ensembles. For instance, the employment of *ab initio* and semi-empirical calculations on the study of several agents, including NAH derivatives [46], has provided interesting aspects on their conformation. However, the conformational preference of a given molecule is not only determined by the lowest energy arrangement of its moieties in vacuum. Consequently, several environmental properties might influence the equilibrium of conformations adopted by such compounds, as hydration and interaction with other biomacromolecules, for which ligand–receptor crystallographic structures are not always available to enlighten the process under study. In fact, it has been proposed that ligands rarely bind to target molecules in their lowest energy conformation [60]. In this context, the present work observed that the conformational preferences of the studied NAH derivatives appear to be influenced by the solvent, resulting in distinct conformational states co-existing in aqueous solutions.

Also, none of such conformations resemble the linear form observed in previous studies in absence of solvent forces [23]. Moreover, considering the higher vasodilatory activity of compound **3**, in comparison to **1**, together with their highly similar exposure of functional groups, it appears to be reasonable to assume that the state "B" may represent or resemble the bioactive conformation of such compounds, at least for their cardiovascular effects, since the relative abundance of conformational state B appears to correlate with the compounds activity.

Upon the characterization of the aqueous conformational ensemble of bioactive compounds, the observer may obtain: (1) information on the conformations present in solution to be selected by the target receptor; (2) the compounds geometries available for conformational induction upon ligand complexation to target receptors; (3) indications on the entropic cost associated to complexation, that is, as higher the conformational complexity of the ligand in solution, less entropically favorable will be the binding process. In docking, the use of solution conformations may contribute in the search for structural data of complexes with higher biological significance, even when using rigid docking.

4. Conclusions

The steps in elucidating the structural basis for compounds pharmacological activity include the identification of both pharmacophoric groups and conformations adopted by such molecules in biological environment. In this context, while a conformational analysis, employing gas phase calculations may provide a minimum energy three-dimensional structure for such molecules, such methods, in most cases, do not evaluate the influence of environmental and temporal properties over the studied compounds. Therefore, the use of such lowest energy conformations as starting geometries in methodologies comprising such terms, as MD simulations, emerges as a promising tool for characterizing the conformational ensemble of bioactive agents in a four-dimensional perspective, that is, considering spatial and temporal properties.

In this context, our results point to a dynamic conformational behavior of NAH derivatives due to solvent effects. As a consequence, depending on the substitution pattern, such compounds may present several conformational states, simultaneously co-existing in water. Since drugs are recognized by its target receptors from aqueous solutions, the knowledge of their conformational ensembles in similar environments is likely to contribute in medicinal chemistry continuous efforts to understand the structural requirements of compounds biological activity.

Acknowledgements

We thank the Conselho Nacional de Desenvolvimento Científico e Tecnológico (CNPq #420015/2005-1 and #472174/2007-0), Fundação Carlos Chagas Filho de Amparo a Pesquisa do Estado do Rio de Janeiro (PRONEX #E-26/171.532/2006), Ministério de Ciência e Tecnologia, the Coordenação de Aperfeiçoamento de Pessoal de Nível Superior (CAPES), Ministério da Educação, Brasília, DF, Brazil, for their financial support and fellowships.

Appendix A. Supplementary data

Supplementary data associated with this article can be found, in the online version, at doi:10.1016/j.jmgm.2009.10.004.

References

[1] C. Humblet, G.R. Marshall, Pharmacophore identification and receptor mapping, Annu. Rep. Med. Chem. 15 (1980) 267–276 (Chapter 28).
[2] A.C. Cunha, J.M. Figueiredo, J.L.M. Tributino, A.L.P. Miranda, H.C. Castro, R.B. Zingali, C.A.M. Fraga, M.C.B.V. de Souza, V.F. Ferreira, E.J. Barreiro, Antiplatelet properties of novel N-substituted-phenyl-1,2,3-triazole-4-acylhydrazone derivatives, Bioorg. Med. Chem. 11 (2003) 2051–2059.
[3] A.C. Cunha, J.L.M. Tributino, A.L.P. Miranda, C.A.M. Fraga, E.J. Barreiro, Synthesis and pharmacological evaluation of novel antinociceptive N-substituted-phenylimidazolyl-4-acylhydrazone derivatives, Il Farmaco 57 (2002) 999–1007.
[4] P.C. Lima, L.M. Lima, K.C. da Silva, P.H. Léda, A.L. de Miranda, C.A.M. Fraga, E.J. Barreiro, Synthesis and analgesic activity of novel N-acylarylhydrazones and isosters, derived from natural safrole, Eur. J. Med. Chem. 35 (2000) 187–203.
[5] G.A. Silva, L.M.M. Costa, F.C.F. Brito, A.L.P. Miranda, E.J. Barreiro, C.A.M. Fraga, New class of potent antinociceptive and antiplatelet 10H-phenothiazine-1-acylhydrazone derivatives, Bioorg. Med. Chem. 12 (2004) 3149–3158.
[6] H.J.C. Bezerra-Neto, D.I. Lacerda, A.L.P. Miranda, H.M. Alves, E.J. Barreiro, C.A.M. Fraga, Design and synthesis of 3,4-methylenedioxy-6-nitrophenoxyacetylhydrazone derivatives obtained from natural safrole: new lead-agents with analgesic and antipyretic properties, Bioorg. Med. Chem. 14 (2006) 7924–7935.
[7] C.D. Duarte, J.L.M. Tributino, D.I. Lacerda, M.V. Martins, M.S. Alexandre-Moreira, F. Dutra, E.J.H. Bechara, F.S. De-Paula, M.O.F. Goulart, J. Ferreira, J.B. Calixto, M.P. Nunes, A.L. Bertho, A.L.P. Miranda, E.J. Barreiro, C.A.M. Fraga, Synthesis, pharmacological evaluation and electrochemical studies of novel 6-nitro-3,4-methylenedioxyphenyl-*N*-acylhydrazone derivatives: discovery of LASSBio-881, a new ligand of cannabinoid receptors, Bioorg. Med. Chem. 15 (2007) 2421–2433.
[8] L.M. Lima, F.S. Frattani, J.L. dos Santos, H.C. Castro, C.A.M. Fraga, R.B. Zingali, E.J. Barreiro, Synthesis and anti-platelet activity of novel arylsulfonateeacylhydrazone derivatives, designed as antithrombotic candidates, Eur. J. Med. Chem. 43 (2008) 348–356.
[9] J.L.M. Tributino, C.D. Duarte, R.S. Corrêa, A.C. Dorigetto, J. Ellena, N.C. Romeiro, N.G. Castro, A.L.P. Miranda, E.J. Barreiro, C.A.M. Fraga, Novel 6-methanesulfonamide-3,4-methylenedioxy-phenyl-*n*-acylhydrazones: orally effective anti-inflammatory drug candidates, Biorg. Med. Chem. 17 (2009) 1125–1131.
[10] A.L.P. Miranda, P.C. Lima, J.L.M. Tributino, P.A. Melo, P.D. Fernandes, W.M. Cintra, C.A.M. Fraga, E.J. Barreiro, Anti-inflammatory, analgesic and anti-platelet properties of LASSBio 294, a new thienylacylhydrazone derivative, in: Abstracts du 6^{éme} Congrès Annuel de la Société Française de Pharmacologie, 2002, p. P296.
[11] R. Li, X. Chen, B. Gong, P.M. Selzer, Z. Li, E. Davidson, G. Kurzban, R.E. Miller, E.O. Nuzum, J.H. McKerrow, R.J. Fletterick, S.A. Gillmor, C.S. Craik, I.D. Kuntz, F.E. Cohen, G.L. Kenyon, Structure-based design of parasitic protease inhibitors, Bioorg. Med. Chem. 4 (1996) 1421–1427.
[12] N. Sluis-Cremer, D. Arion, M.A. Parniak, Destabilization of the HIV-1 reverse transcriptase dimer upon interaction with *N*-acyl hydrazone inhibitors, Mol. Pharmacol. 62 (2002) 398–405.
[13] J.R. Dimmock, G.B. Baker, W.G. Taylor, Arylhydrazones. Part II. The ultraviolet spectroscopy and antimicrobial evaluation of some substituted aroylhydrazones, Can. J. Pharm. Sci. 7 (1972) 100–103.
[14] R.T. Sudo, G. Zapata-Sudo, E.J. Barreiro, The new compound, LASSBio 294, increases the contractility of intact and saponin-skinned cardiac muscle from Wistar rats, Br. J. Pharmacol. 134 (2001) 603–613.
[15] H. Gonzalez-Serratos, R. Chang, E.F. Pereira, N.G. Castro, Y. Aracava, P.A. Melo, P.C. Lima, C.A.M. Fraga, E.J. Barreiro, E.X. Albuquerque, A novel thienylhydrazone, (2-thienylidene)3,4-methylenedioxybenzoylhydrazine, increases inotropism and decreases fatigue of skeletal muscle, J. Pharmacol. Exp. Ther. 229 (2001) 558–566.
[16] C.L.M. Silva, F. Noël, E.J. Barreiro, Cyclic GMP-dependent vasodilatory properties of LASSBio 294 in rat aorta, Br. J. Pharmacol. 135 (2002) 293–298.
[17] G. Zapata-Sudo, R.T. Sudo, P.A. Maronas, G.L. Silva, O.R. Moreira, M.I. Aguiar, E.J. Barreiro, Thienylhydrazone derivative increases sarcoplasmic reticulum Ca^{2+} release in mammalian skeletal muscle, Eur. J. Pharmacol. 470 (2003) 79–85.
[18] A.G. Silva, G. Zapata-Sudo, A.E. Kummerle, C.A.M. Fraga, E.J. Barreiro, R.T. Sudo, Synthesis and vasodilatory activity of new *N*-acylhydrazone derivatives, designed as LASSBio-294 analogues, Bioorg. Med. Chem. 13 (2005) 3431–3437.
[19] K.M. Sureshan, T. Miyasou, Y. Watanake, Crystal structure of 1L-1,2:4,5-di-O-isopropylidene-allo-inositol; a comparison of its conformation in solid and solution states, Carbohydr. Res. 339 (2004) 1551–1555.
[20] C.R. Søndergaard, A.E. Garrett, T. Carstensen, G. Pollastri, J.E. Nielsen, Structural artifacts in protein–ligand X-ray structures: implications for the development of docking scoring functions, J. Med. Chem. 52 (2009) 5673–5684.
[21] A.R. Leach, Conformational analysis, in: A.R. Leach (Ed.), Molecular Modeling Principles and Applications, Pearson Education Limited, London, 2001, pp. 457–508.
[22] W.F. van Gunsteren, H.J.C. Berendsen, Computer simulation of molecular dynamics: methodology, applications, and perspectives in chemistry, Angew. Chem. Int. Ed. Engl. 29 (1990) 992–1023.
[23] A.E. Kummerle, J.M. Raimundo, C.M. Leal, G.S. da Silva, T.L. Balliano, M.A. Pereira, C.A. de Simone, R.T. Sudo, G. Zapata-Sudo, C.A.M. Fraga, E.J. Barreiro, Studies towards the identification of putative bioactive conformation of potent vasodilator arylidene *N*-acylhydrazone derivatives, Eur. J. Med. Chem. 44 (2009) 4004–4009.
[24] A.W. Schuettelkopf, D.M.F. van Aalten, PRODRG: a tool for high-throughput crystallography of protein–ligand complexes, Acta Crystallogr. Sect. D 60 (2004) 1355–1363.
[25] M.W. Schmidt, K.K. Baldridge, J.A. Boatz, S.T. Elbert, M.S. Gordon, J.H. Jensen, S. Koseki, N. Matsunaga, K.A. Nguyen, S.J. Su, T.L. Windus, M. Dupuis, J.A. Montgomery, General atomic and molecular electronic structure system, J. Comput. Chem. 14 (1993) 1347–1363.
[26] MOPAC2009, version 9.211, Stewart Computational Chemistry, Colorado Springs, CO, USA, 2008.

[27] G. Schaftenaar, J.H. Noordik, Molden: a pre- and post-processing program for molecular and electronic structures, J. Comput.-Aided Mol. Design 14 (2000) 123–134.
[28] D. van der Spoel, E. Lindahl, B. Hess, G. Groenhof, A.E. Mark, H.J.C. Berendsen, GROMACS: fast, flexible, and free, J. Comput. Chem. 26 (2005) 1701–1718.
[29] W.F. van Gunsteren, S.R. Billeter, A.A. Eising, P.H. Huenenberger, P. Krueger, A.E. Mark, W.R.P. Scott, I.G. Tironi, Biomolecular Simulation: The GROMOS96 Manual and User Guide, Vdf Hochschulverlag, AG Zurich, Switzerland, 1996.
[30] C.M.R. Sant'Anna, R.B. de Alencastro, E.J. Barreiro, Toward a platelet-activating factor pseudoreceptor. 2. Three-dimensional semiempirical models for agonist and antagonist binding, J. Mol. Struct.-Theochem. 490 (1999) 167–180.
[31] G.B. Rocha, R.O. Freire, A.M. Simas, J.J.P. Stewart, RM1: a reparameterization of AM1 for H, C, N, O, P, S, F, Cl, Br, and I, J. Comput. Chem. 27 (2006) 1101–1111.
[32] E.P. Peçanha, H. Verli, C.R. Rodrigues, E.J. Barreiro, C.A.M. Fraga, Highly diastereoselective mercury-mediated synthesis of functionalized 2-azabicyclo[3.3.0]octane derivatives, Tetrahedr. Lett. 43 (2002) 1607–1611.
[33] C.L. Cardoso, D.H.S. Silva, D.M. Tomazela, H. Verli, M.C.M. Young, M. Furlan, M. Eberlin, V.S. Bolzani, Turbinatine, a potential key intermediate in the biosynthesis of corynanthean-type indole alkaloids, J. Nat. Prod. 66 (2003) 1017–1021.
[34] O. Flausino Jr., L.A. Santos, H. Verli, A.M. Pereira, V.S. Bolzani, R.L. Nunes-de-Souza, Anxiolytic effects of erythrinian alkaloids from *Erythrina mulungu*, J. Nat. Prod. 70 (2007) 48–53.
[35] V.A. Kerber, C.S. Passos, H. Verli, A.G. Fett-Neto, J.P. Quirion, A.T. Henriques, Psychollatine, a glucosidic monoterpene indole alkaloid from *Psychotria umbellate*, J. Nat. Prod. 71 (2008) 697–700.
[36] J.J.P. Stewart, Optimization of parameters for semiempirical methods V: modification of NDDO approximations and application to 70 elements, J. Mol. Model. 13 (2007) 1173–1213.
[37] A. Klamt, G. Schüürman, COSMO: a new approach to dielectric screening in solvents with explicit expressions for the screening energy and its gradient, J. Chem. Soc. Perkin Trans. 2 (1993) 799–805.
[38] H. Verli, J.A. Guimarães, Molecular dynamics simulation of a decasaccharide fragment of heparin in aqueous solution, Carbohydr. Res. 339 (2004) 281–290.
[39] C.F. Becker, J.A. Guimarães, H. Verli, Molecular dynamics and atomic charge calculations in the study of heparin conformation in aqueous solution, Carbohydr. Res. 340 (2005) 1499–1507.
[40] L. Pol-Fachin, H. Verli, Depiction of the forces participating in the 2-O-sulfo-alpha-L-iduronic acid conformational preference in heparin sequences in aqueous solutions, Carbohydr. Res. 343 (2008) 1435–1445.
[41] H.J.C. Berendsen, J.R. Grigera, P. Straatsma, The missing term in effective pair potentials, J. Phys. Chem. 91 (1987) 6269–6271.
[42] B.L. de Groot, H. Grubmüller, Water permeation across biological membranes: mechanism and dynamics of aquaporin-1 and GlpF, Science 294 (2001) 2353–2357.
[43] T. Darden, D. York, L. Pedersen, Particle mesh Ewald—an $N\log(N)$ method for Ewald sums in large systems, J. Chem. Phys. 98 (1993) 10089–10092.
[44] B. Hess, H. Bekker, H.J.C. Berendsen, J.G.E.M. Fraaije, LINCS: a linear constraint solver for molecular simulations, J. Comput. Chem. 18 (1997) 1463–1472.
[45] H.J.C. Berendsen, J.P.M. Postma, A. DiNola, J.R. Haak, Molecular dynamics with coupling to an external bath, J. Chem. Phys. 81 (1984) 3684–3690.
[46] D.R. Ifa, C.R. Rodrigues, R.B. de Alencastro, C.A.M. Fraga, E.J. Barreiro, A possible molecular mechanism for the inhibition of cysteine proteases by salicylaldehyde *N*-acylhydrazones and related compounds, J. Mol. Struct.-Theochem. 505 (2000) 11–17.
[47] A. Szymoszek, A. Koll, Internal rotation in ortho-chloro-substituted biphenyls. Ab initio and molecular dynamics study, Chem. Phys. Lett. 373 (2003) 591–598.
[48] S. Fischer, C.S. Verma, Binding of buried structural water increases the flexibility of proteins, Proc. Natl. Acad. Sci. U.S.A. 96 (1999) 9613–9615.
[49] R.U. Lemieux, How water provides the impetus for molecular recognition in aqueous solution, Acc. Chem. Res. 29 (1996) 373–380.
[50] D. Kosztin, R.I. Gumport, K. Schulten, Probing the role of structural water in a duplex oligodeoxyribonucleotide containing a water-mimicking base analog, Nucleic Acids Res. 27 (1999) 3550–3556.
[51] S.P. Kanaujia, K. Sekar, Structural and functional role of water molecules in bovine pancreatic phospholipase A_2: a data-mining approach, Acta Cryst. D 65 (2009) 74–84.
[52] A. De Simone, G.G. Dodson, C.S. Verma, A. Zagari, F. Fraternali, Prion and water: tight and dynamical hydration sites have a key role in structural stability, Proc. Natl. Acad. Sci. U.S.A. 102 (2005) 7535–7540.
[53] C. Andersson, S.B. Engelsen, The mean hydration of carbohydrates as studied by normalized two dimensional radial pair distributions, J. Mol. Graph. Model. 17 (1999) 101–105.
[54] E.R. Caffarena, A.C. Lorenzo, Conformational and dynamical properties of the niruriside in aqueous solution: a molecular dynamics approach, J. Mol. Struct.-Theochem. 714 (2005) 189–197.
[55] K.A. Brameld, B. Kuhn, D.C. Reuter, M. Stahl, Small molecule conformational preferences derived from crystal structure data. A medicinal chemistry focused analysis, J. Chem. Inform. Model. 48 (2008) 1–24.
[56] C.M. Lanthier, M.A. Parniak, G.I. Dmitrienko, Inhibition of carboxypeptidase a by n-(4-t-butylbenzoyl)-2-hydroxy-1-naphthaldehyde hydrazone, Bioorg. Med. Chem. Lett. 7 (1997) 1557–1562.
[57] D. Arion, N. Sluis-Cremer, K.L. Min, M.E. Abram, R.S. Fletcher, M.A. Parniak, Mutational analysis of Tyr-501 of HIV-1 reverse transcriptase, J. Biol. Chem. 277 (2002) 1370–1374.
[58] M.F. Simeonov, F. Fulop, R. Sillanpaa, K. Pihlaja, Conformational complexity in seven-membered cyclic triazepinone/open hydrazones. 2. Molecular modeling and X-ray study, J. Org. Chem. 62 (1997) 5089–5095.
[59] H.-J. Böhm, G. Klebe, What can we learn from molecular recognition in protein–ligand complexes for the design of new drugs? Angew. Chem. Int. Ed. 35 (1996) 2588–2614.
[60] E. Perola, P.S. Charifson, Conformational analysis of drug-like molecules bound to proteins: an extensive study of ligand reorganization upon binding, J. Med. Chem. 47 (2004) 2499–2510.